11-9-2007

Microwave Spectra and ab Initio Studies of Ar-Propane and Ne-Propane Complexes: Structure and Dynamics

Karen I. Peterson

David Pullman

Wei Lin
The University of Texas Rio Grande Valley, wei.lin@utrgv.edu

Andrea J. Minei

Stewart E. Novick

Recommended Citation

Peterson, K. I., Pullman, D., Lin, W., Minei, A. J., & Novick, S. E. (2007). Microwave spectra and ab initio studies of Ar-propane and Ne-propane complexes: Structure and dynamics. The Journal of Chemical Physics, 127(18), 184306. https://doi.org/10.1063/1.2780775

The Journal of Chemical Physics

Microwave spectra and *ab initio* studies of Ar-propane and Ne-propane complexes: Structure and dynamics

Cite as: J. Chem. Phys. **127**, 184306 (2007); https://doi.org/10.1063/1.2780775
Submitted: 17 July 2007 . Accepted: 15 August 2007 . Published Online: 09 November 2007

Karen I. Peterson, David Pullman, Wei Lin, Andrea J. Minei, and Stewart E. Novick

Microwave spectra and *ab initio* studies of Ar-propane and Ne-propane complexes: Structure and dynamics

Karen I. Peterson and David Pullman
Department of Chemistry, San Diego State University, San Diego, California 92182-1030, U.S.A.

Wei Lin,[a] Andrea J. Minei, and Stewart E. Novick
Department of Chemistry, Wesleyan University, Middletown, Connecticut 06459, U.S.A.

(Received 17 July 2007; accepted 15 August 2007; published online 9 November 2007)

Microwave spectra in the 7–26 MHz region have been measured for the van der Waals complexes, $Ar–CH_3CH_2CH_3$, $Ar–^{13}CH_3CH_2CH_3$, $^{20}Ne–CH_3CH_2CH_3$, and $^{22}Ne–CH_3CH_2CH_3$. Both *a*- and *c*-type transitions are observed for the Ar-propane complex. The *c*-type transitions are much stronger indicating that the small dipole moment of the propane (0.0848 D) is aligned perpendicular to the van der Waals bond axis. While the 42 transition lines observed for the primary argon complex are well fitted to a semirigid rotor Hamiltonian, the neon complexes exhibit splittings in the rotational transitions which we attribute to an internal rotation of the propane around its *a* inertial axis. Only *c*-type transitions are observed for both neon complexes, and these are found to occur between the tunneling states, indicating that internal motion involves an inversion of the dipole moment of the propane. The difference in energy between the two tunneling states within the ground vibrational state is 48.52 MHz for $^{20}Ne–CH_3CH_2CH_3$ and 42.09 MHz for $^{22}Ne–CH_3CH_2CH_3$. The Kraitchman substitution coordinates of the complexes show that the rare gas is oriented above the plane of the propane carbons, but shifted away from the methylene carbon, more so in Ne propane than in Ar propane. The distance between the rare gas atom and the center of mass of the propane, R_{cm}, is 3.823 Å for Ar-propane and 3.696 Å for Ne-propane. *Ab initio* calculations are done to map out segments of the intermolecular potential. The global minimum has the rare gas almost directly above the center of mass of the propane, and there are three local minima with the rare gas in the plane of the carbon atoms. Barriers between the minima are also calculated and support the experimental results which suggest that the tunneling path involves a rotation of the propane subunit. The path with the lowest effective barrier is through a C_{2v} symmetric configuration in which the methyl groups are oriented toward the rare gas. Calculating the potential curve for this one-dimensional model and then calculating the energy levels for this potential roughly reproduces the spectral splittings in Ne-propane and explains the lack of splittings in Ar-propane. © *2007 American Institute of Physics*. [DOI: 10.1063/1.2780775]

I. INTRODUCTION

The structure and dynamics of many complexes have been analyzed spectroscopically, but there are certain limitations and it is becoming increasingly clear that we will have to rely on *ab initio* calculations to aid in the interpretation of experimental results and, perhaps, even to replace them. Complexes involving alkanes are prime examples for which the feasibility of experimental studies is uncertain because of low dipole moments, weak interactions, and spectral complexity. Even the simple propane dimer is probably invisible to the microwave spectroscopist—*ab initio* calculations have found that the minimum energy structure has a zero dipole moment. If we are going to use *ab initio* calculations in place of experimental results, we need to be confident of their reliability. The increase of desktop computing capability has made high-level structural calculations of van der Waals complexes more readily available to the experimentalist, opening the way for a useful synthesis of theory and experiment. Recently, Jäger and co-workers have taken this approach in their studies of $Ar–CH_4$, $Kr–CH_4$, and $Xe–CH_4$.[1,2] They were able to combine high-level *ab initio* calculations with high resolution microwave spectroscopy to illuminate the effects of the anisotropy of the interaction potential. One conclusion derived from their work is that the rare gas tends to orient itself in a position which maximizes its interaction with the most polarizable part of the methane—the carbon atom. Unfortunately, since the methane molecule undergoes almost free internal motion within the complex, a direct comparison between the theoretical and experimental results was limited. Rare gas complexes with ethane would likely exhibit the same difficulties, but propane, with its bent structure, could be more restricted, thereby simplifying the results. Since it is evident that atomic polarizability is an important component in the rare gas interactions, we would expect that a rare gas atom (Rg) would bind to the propane in such a way as to minimize the distance between all three carbon atoms, that is, above the plane defined by the carbon atoms. In fact, as we report in this

[a]Present address: Department of Chemistry, University of Saint Mary, Leavenworth, KS 66048, USA.

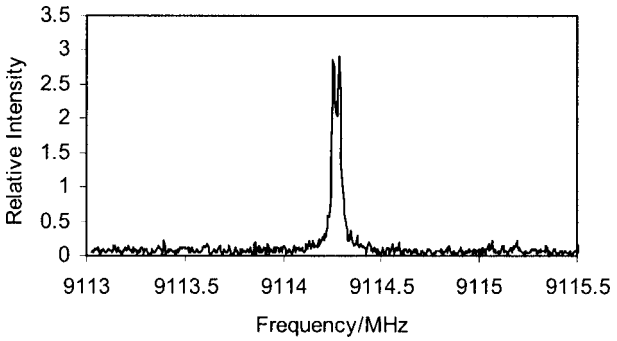

FIG. 1. The 1_{10}-0_{00} transition of Ar–C_3H_8 averaged over 1000 pulses. The peak is split by Doppler shifting.

paper, this is the case for Rg-propane, and we are able to evaluate more directly *ab initio* calculations with an experimentally derived structure.

At its equilibrium geometry, the propane molecule has C_{2v} symmetry. Each methyl group has one hydrogen atom which is coplanar with the carbon atoms, directed away from the C_2 axis.[3] The methyl groups encounter a relatively high internal rotation barrier of about 1100 cm^{-1}, so the spectral splittings caused by this motion are not expected to be observed in a van der Waals complex. A much lower barrier is expected for an internal rotation of the propane relative to the rare gas atom since the intermolecular interaction is weak, but the motion involves heavy off-axis atoms so the splittings caused by this motion could also be too small to be observed. Although we find no evidence for this internal motion in Ar-propane, it is clearly exhibited by relatively large splittings observed in Ne-propane.

In this paper, we report the experimentally derived structures of Ar-propane and Ne-propane and present results pertaining to the dynamics within the complexes. *Ab initio* calculations are also done both to help interpret the observed results and to determine the level of theory required to accurately describe the geometry and energetics of a weakly bound complex.

II. EXPERIMENT

The microwave spectra of Ar–C_3H_8, Ar–$^{13}C_3H_8$, ^{20}Ne–C_3H_8, and ^{22}Ne–C_3H_8 were measured using the pulsed jet Fourier transform microwave spectrometer constructed at Wesleyan University.[4] This spectrometer, described in detail previously, has been upgraded with improved microwave circuitry and automated scanning capability. In addition, the pulsed jet, which was originally set to expand perpendicularly into the microwave cavity, is now positioned to expand coaxially. This increases the sensitivity because of the longer residence time of the complexes in the cavity. The resolution is also greatly increased because the Doppler broadening, which occurred in the original jet configuration, is minimized. Instead, a frequency-dependent Doppler shifting doubles the lines. For example, the 1_{10}-0_{00} transition of Ar–C_3H_8 at 9114 MHz, shown in Fig. 1, is shifted by approximately ±15 kHz. The reported frequencies are the average of the two Doppler components.

The pulsed jet expansion conditions were typical for weakly bound complexes. To synthesize Ar–C_3H_8 and Ar–$^{13}C_3H_8$ complexes, a 1% mixture of propane in argon was expanded through a 0.5 mm pulsed nozzle with a backing pressure of about 0.7 atm. A set of 42 transitions were assigned to Ar–C_3H_8 and five transitions were observed for naturally abundant Ar–$^{13}C_3H_8$. We also observed known transitions of H_2O-propane and Ar–H_2O transitions due to residual H_2O in the gas line. The microwave cavity into which the gas was expanded was tunable between 5 and 26.5 GHz. Although we did not measure the dipole moment, crude evaluations of the dipole moments could be made by noting the effects of changing the microwave power on the individual transitions. Thus, we found that while the H_2O complexes could be observed at low power, the Ar-propane transitions required very high power, as would be expected for a complex with a low dipole moment. The dipole moment of propane is only 0.0848 D,[5] and the induced dipole moment within such a weakly bound complex is expected to be much less than 0.1 D.

^{20}Ne–C_3H_8 and ^{22}Ne–C_3H_8 complexes were observed by using a mixture of 0.5% propane in neon with a backing pressure of about 2 atm. The signal intensities of the transitions were much lower than those of Ar–C_3H_8, as would be expected for a more weakly bound and, thus, less populated complex. Even with the lower intensities, ^{22}Ne–C_3H_8 transitions could be observed because of the relatively high natural abundance of ^{22}Ne (8.9%).

III. SPECTROSCOPIC RESULTS

The transitions observed for Ar-propane are listed in Table I. The transitions are fitted with the following Watson "*S*" reduction Hamiltonian[6] in a $\mathbf{I}^r$-representation using the SPFIT fitting program of Pickett,[7]

$$H = AJ_a^2 + BJ_b^2 + CJ_c^2 - D_J J^4 - D_K J_a^4 - D_{JK} J^2 J_a^2 + d_1 J^2 (J_+^2 + J_-^2) + d_2 (J_+^4 + J_-^4) + H_{JK} J^4 J_a^2. \quad (1)$$

With 9 constants, the 42 lines of the Ar–C_3H_8 are fitted with a standard deviation of 2.5 kHz. The fitted constants are given in Table II. Five transitions are observed for the isotopomer Ar–$^{13}C_3H_8$ in natural abundance, and these are listed in Table III. The Ar–$^{13}C_3H_8$ transitions are fitted by setting the quartic constants equal to those obtained for Ar–$^{12}C_3H_8$. The resulting rotational constants are given in Table III. We assume that these rotational constants correspond to Ar–$^{13}CH_3CH_2CH_3$ rather than Ar–$CH_3{}^{13}CH_2CH_3$ because our structural evaluation is more consistent with this identification and, also, because the former complex is twice as abundant. We looked extensively for another isotopomer, but the transitions were too weak to be observed.

In general, the *c*-type transitions are much stronger than the *a*-type transitions, implying that the dipole moment along the van der Waals bond axis is much smaller than that along the *c* axis of the complex. This suggests that the propane symmetry axis is parallel to the *c* axis of the complex [see Fig. 2(a)] since propane has a dipole moment in that direction. Since argon is very weakly bound to propane, the propane molecule is expected to encounter a relatively low bar-

TABLE I. Observed transitions for Ar–C_3H_8.

$J'_{K_aK_c}$-$J''_{K_aK_c}$	ν (MHz)[a]	$J'_{K_aK_c}$-$J''_{K_aK_c}$	ν (MHz)[a]
a-type transitions		c-type transitions	
3_{13}-2_{12}	8 530.016(−4)	5_{05}-4_{13}	7 536.009(1)
3_{03}-2_{02}	8 795.468(0)	1_{10}-0_{00}	9 114.269(4)
3_{12}-2_{11}	9 088.250(−2)	6_{06}-5_{14}	9 879.456(5)
4_{14}-3_{13}	11 367.676(−2)	2_{21}-3_{13}	9 999.294(0)
4_{04}-3_{03}	11 706.532(2)	7_{07}-6_{15}	12 060.879(5)
4_{23}-3_{22}	11 741.938(−2)	2_{11}-1_{01}	12 237.504(4)
4_{13}-3_{12}	12 111.469(1)	3_{12}-2_{02}	15 454.660(2)
5_{15}-4_{14}	14 200.649(−1)	6_{25}-6_{15}	16 319.030(1)
5_{05}-4_{04}	14 600.137(2)	5_{24}-5_{14}	16 864.137(−1)
5_{14}-4_{13}	15 129.189(−1)	4_{23}-4_{13}	17 322.732(−5)
6_{16}-5_{15}	17 027.982(−4)	3_{22}-3_{12}	17 692.258(−2)
6_{06}-5_{05}	17 472.635(1)	2_{21}-2_{11}	17 970.865(−2)
6_{25}-5_{24}	17 594.714(4)	2_{20}-2_{12}	18 533.570(0)
6_{24}-5_{23}	17 741.070(−4)	4_{13}-3_{03}	18 770.659(1)
6_{15}-5_{14}	18 139.820(0)	3_{21}-3_{13}	18 830.205(0)
7_{17}-6_{16}	19 848.870(−8)	4_{22}-4_{14}	19 246.882(2)
7_{07}-6_{06}	20 321.243(1)	5_{23}-5_{15}	19 801.221(3)
7_{26}-6_{25}	20 513.390(1)	6_{24}-6_{16}	20 514.307(2)
7_{16}-6_{15}	21 141.607(−1)	7_{25}-7_{17}	21 409.685(0)
		5_{14}-4_{04}	22 193.317(−1)
		2_{20}-1_{10}	24 036.142(−2)
		2_{21}-1_{11}	24 218.053(0)
		6_{15}-5_{05}	25 733.002(0)

[a]Numbers in parentheses are $\nu_{obs}-\nu_{calc}$.

rier to an internal motion. If the barrier is low enough, we would expect to see a second set of transitions offset by an amount related to the height of the barrier. Although we do not see additional transitions for Ar-propane, these were observed for Ne-propane. This is similar to the spectra observed for rare gas–cyclopropane complexes.[8]

Two sets of *c*-type transitions, separated by 65–90 MHz, could be definitively assigned for each of the Ne-propane complexes and these are listed in Table IV. The doubling of each transition is indicative of the presence of an internal motion which splits each rotational level into lower and upper tunneling states. Depending on the relevant internal motion, transitions could be within a tunneling state or between tunneling states. We found that the best fit occurred with *c*-type transitions allowed between the tunneling states. The $v=0$ and $v=1$ energy levels were calculated using separate semirigid rotor Hamiltonians, offset from each other by ΔE. Transitions between these levels were fit to the observed transitions. No coupling between the two states was necessary for a good fit.

TABLE II. Spectroscopic constants (in MHz) for Ar–C_3H_8.

A	7552.4371 (37)
B	1561.99691 (48)
C	1375.82266 (38)
D_J	$8.5501(48)\times10^{-3}$
D_{JK}	0.12132 (10)
D_K	−0.1125(7)
d_1	$-1.0647(30)\times10^{-3}$
d_2	$-0.3022(21)\times10^{-3}$
H_{JK}	$-0.0183(18)\times10^{-3}$
rms (kHz)	2.5

TABLE III. Rotational transitions and spectroscopic constants (in MHz) for Ar–$^{13}CH_3CH_2CH_3$. The distortion constants are set equal to those obtained for Ar–C_3H_8.

$J'_{K_aK_c}$-$J''_{K_aK_c}$	ν (MHz)[a]
1_{10}-0_{00}	8918.682(4)
2_{11}-1_{01}	12011.397(0)
3_{12}-2_{02}	15199.228(−5)
4_{13}-3_{03}	18487.372(3)
3_{21}-3_{13}	18346.248(0)
A	7372.1076(71)
B	1546.7393(12)
C	1358.3416(30)
rms (kHz)	3

[a]Numbers in parentheses are $\nu_{obs}-\nu_{calc}$.

$$H_{v=0} = AJ_a^2 + BJ_b^2 + CJ_c^2 - D_J J^4,$$
$$H_{v=1} = A'J_a^2 + B'J_b^2 + C'J_c^2 - D'_J J^4 + \Delta E. \quad (2)$$

For ^{20}Ne-propane, we set $C=C'$ and $D_J=D'_J$, so that the ten transitions were fit with seven parameters. Only six transitions were observed for ^{22}Ne-propane, so we set $A=A'$ and $C=C'$. Furthermore, to limit ourselves to five parameters, both D_J and D'_J were set to be equal to that of ^{20}Ne-propane (see Table V).

An energy level diagram showing the observed *c*-type transitions of ^{20}Ne-propane is given in Fig. 3. Also shown are the predicted *a*-type transitions. Only *c*-type transitions were observed because of the low overall signal intensity. Both the concentration of Ne-propane in the beam and the dipole moment of Ne-propane along the *a* axis are expected to be smaller than for Ar-propane because of the lower polarizability of the Ne atom. Notice that the *a*-type transitions occur within each set of internal rotor states. Group theoretical arguments discussed later in this paper support this prediction.

IV. STRUCTURAL ANALYSIS

A. Argon-propane complexes

For most weakly bound binary complexes, the *a* inertial axis is aligned quite closely with the line connecting the

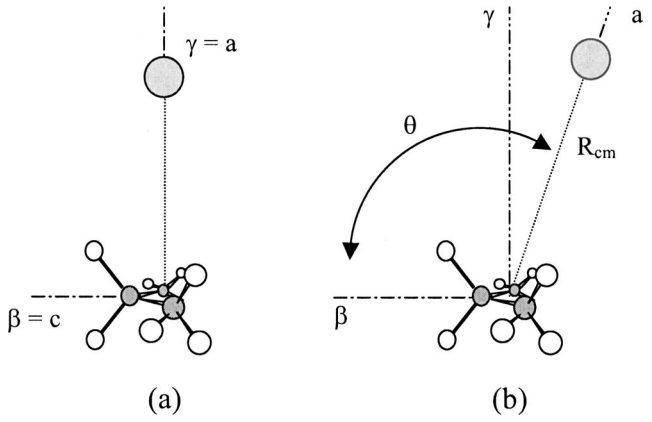

FIG. 2. (a) Diagram in which the inertial axes of the propane, α, β, and γ, are parallel to the axes of the complex, *a*, *b*, and *c*. In this case, $I_a=I_\gamma$. (b) Diagram of the structure of Ar propane derived from Kraitchman's substitution method. θ is the angle between the van der Waals bond axis (which is approximately equal to the *a* axis of the complex) and the β axis of propane.

TABLE IV. Observed transitions for $Ne-C_3H_8$.

	ν (MHz)[a]			
$J'_{K_aK_c}$-$J''_{K_aK_c}$	$A' \leftarrow B''$	$B' \leftarrow A''$	Center (MHz)	Δ (MHz)
$^{20}Ne-C_3H_8$				
1_{10}-0_{00}	10 190.526(−10)	10 182.625(−4)	10 137.076	91.099
2_{11}-1_{01}	15 012.653(13)	15 098.445(19)	15 055.549	86.798
3_{12}-2_{02}	20 160.424(−1)	20 237.794(−26)	20 199.109	77.370
4_{13}-3_{03}	25 563.698(−2)	25 630.023(10)	25 596.861	66.325
2_{20}-2_{12}	16 951.463(0)	17 022.591(0)	16 987.027	71.128
$^{22}Ne-C_3H_8$				
1_{10}-0_{00}	9 953.899(5)	10 036.998(−5)	9 995.449	83.099
2_{11}-1_{01}	14 599.069(−9)	14 677.939(9)	14 638.504	78.870
3_{13}-2_{02}	19 447.135(3)	19 519.253(−3)	19 483.194	72.11

[a]Numbers in parentheses are $\nu_{obs}-\nu_{calc}$.

centers of mass of the two subunits. When one of the subunits is an atom, as is the case for Rg-propane, the moment of inertia around the a axis, I_a, is predominantly due to the inertial tensor of the molecular subunit rotated in the axis system of the complex. From the measured rotational constants of propane, given in Table VI, we see that C is only about 100 MHz different from the A rotational constant of Ar-propane. The fact that these two constants are similar indicates that the c axis of propane is approximately aligned with the a axis of the complex. This results in a structure with the argon atom above the plane of propane carbons, which is in agreement with the difference in transition strengths observed for the a-and c-type transitions. A structure in which the axis system of the complex is aligned with that of propane is shown in Fig. 2(a). To avoid confusion, we will use α, β, and γ to symbolize the a, b, and c axes of propane.

A more refined structural determination can be made by using Kraitchman's method,[9] which compares the moments of inertia of an isotopically substituted compound with those of the parent species to calculate the absolute value of the position of the isotopically substituted atom. Even though only one Ar isotope is observed, the position of the argon atom relative to the propane can be found by comparing the rotational constants of propane and of Ar-propane, where propane is taken as the parent species. This effectively corresponds to an isotopic substitution of the argon atom from a mass of 0 amu to a mass of 39.962 amu. See Refs. 10 and 11 for more details about this procedure. The resulting coordinates for the argon atom in the propane principal axis system are $(x_\alpha, x_\beta, x_\gamma) = (0.23i$ Å, 1.375 Å, 3.575 Å). The imaginary value for x_α arises from the fact that the square of x_α, which is the parameter calculated by Kraitchman's equation, is negative. This nonphysical result is representative of the unreliability of Kraitchman's method for small coordinates involved in large amplitude motions[12] and leads us to suspect that the equilibrium value of x_α is close to zero.

Figure 2(b) shows the structure of the Ar-propane complex with the argon atom positioned at the coordinates calculated from Kraitchman's method. Since this method gave an imaginary value of x_α, x_α was set equal to zero, locating

TABLE V. Spectroscopic constants for $^{20}Ne-C_3H_8$ and $^{22}Ne-C_3H_8$ in MHz.

	$^{20}Ne-C_3H_8$		$^{22}Ne-C_3H_8$	
	$v=0$	$v=1$	$v=0$	$v=1$
A	7679.711 (27)	7675.086 (27)	7673.461 (17)[b]	
B	2460.531 (16)	2459.205 (16)	2322.703 (8)	2321.639 (8)
C	2023.792 (25)[b]		1929.39 (6)[b]	
D_J	0.04593 (64)[b]		0.04593[a]	
ΔE	48.522 (16)		42.087 (10)	
rms (kHz)	48		6	

[a]This value was set equal to the fitted value for $^{20}Ne-C_3H_8$.
[b]Only one value was fitted. Both internal states were assumed to have the same value.

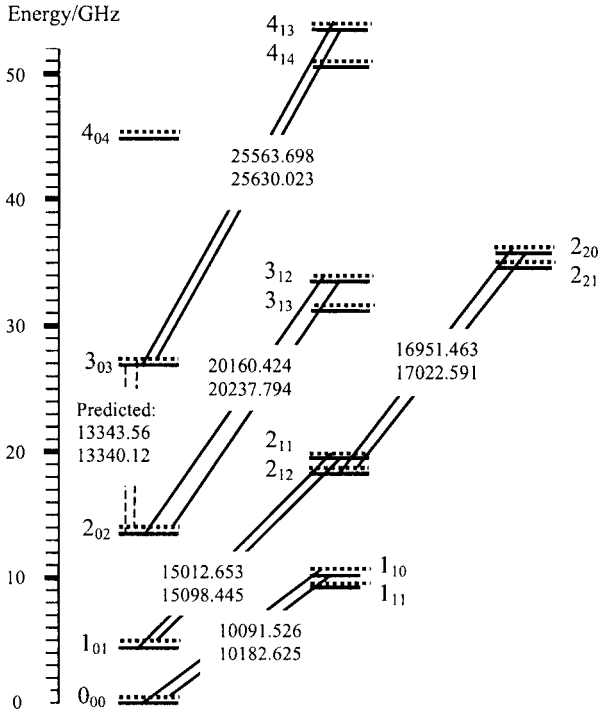

FIG. 3. Ne-propane energy level diagram. Transition frequencies are given in MHz. The solid horizontal lines show the $v=0$ internal state and the dotted lines show the $v=1$ internal rotor state. The energy difference between the two states is exaggerated to about ten times the actual difference.

TABLE VI. Rotational constants for C_3H_8 and $^{13}CH_3CH_2CH_3$ in MHz (Ref. 3).

	$CH_3CH_2CH_3$	$^{13}CH_3CH_2CH_3$
A	29 207.36	29 092.05
B	8 446.07	8 228.77
C	7 458.98	7 281.73

the argon atom within the propane symmetry plane. From the values of x_β and x_γ, the distance between the centers of mass, R_{cm}, is calculated to be 3.83 Å, and the angle θ between the propane β axis and the van der Waals bond axis [see Fig. 2(b)] is either 69° or 111°. Notice that a value of $\theta=111°$ positions the methyl-group carbons toward the argon atom (relative to the *bc* plane of the complex), but $\theta=69°$ positions them away from the argon. The value of θ can be established with the additional information available in the rotational constants of the isotopically substituted species, $Ar-^{13}CH_3CH_2CH_3$. Comparing these constants with those of the parent species $Ar-C_3H_8$, the coordinates for the ^{13}C position in the principal axis system of the complex are calculated to be $(x_a,x_b,x_c)=(1.774,1.272,0.229)$. It is comforting to note that x_b is equal to one-half the distance between the outer carbon atoms in propane (perhaps somewhat fortuitously) since this agrees with the assumption that the argon is located in the bisecting symmetry plane of the propane. The coordinate x_a is the best gauge of the angle θ; it should be equal to 1.82 Å if the outer carbons are in the *bc* plane of the complex (1.82 Å is the distance between the propane center of mass and the complex center of mass). The fact that x_a is less than 1.82 Å implies that the outer carbons are oriented toward the argon atom and, therefore, $\theta=111°$, as shown in Fig. 2(b).

Since Kraitchman's method gives an unsatisfactory result for x_α, it is useful to calculate a set of rotational constants from the proposed atomic coordinates and compare these directly with the experimental constants. This was done, in the manner described by Suenram *et al.* for the Ar–formamide complex,[14] by setting up an inertial tensor in the (x,y,z) frame in terms of the moments of inertia of the propane and a pseudodiatomic moment of inertia for the complex, μR_{cm}^2, where $\mu=m_{propane}m_{Ar}/(m_{propane}+m_{Ar})$. The polar coordinate system used for this calculation is given in Fig. 4. As before, θ is the angle between the symmetry axis of the propane and the van der Waals bond axis (*a* axis) of the complex. φ is the projection of the van der Waals bond axis onto the $\alpha\gamma$ axis plane of the propane.

The Kraitchman coordinates for argon $(x_\alpha,x_\beta,x_\gamma)=(0\text{ Å},1.375\text{ Å},3.575\text{ Å})$ correspond to the polar coordinates, $(R_{cm},\theta,\varphi)=(3.830\text{ Å},111°,0°)$. The moments of inertia of propane needed to calculate the inertial tensor are derived from the rotational constants given in Table VI. Diagonalizing the inertial tensor gives the principal moments of inertia of the complex from which rotational constants can be calculated; these are given in the second column of Table VII. As expected, the agreement is not particularly good because we had to assume that $x_\alpha=0$ ($\varphi=0°$), so we next varied R_{cm}, θ, and φ until the difference between the observed and calculated constants was minimized. The new effective coordinates are $(R_{cm},\theta,\varphi)=(3.823\text{ Å},108.7°,0.5°)$. The rotational constants of $Ar-^{13}CH_3CH_2CH_3$ were calculated with both the original substitution coordinates and the refined coordinates. The agreement again is much improved for the latter, and this increases our confidence in the structural determination.

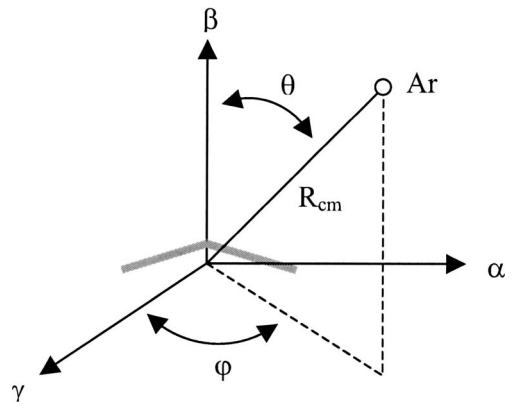

FIG. 4. The polar coordinate system used in this paper. The propane molecule is oriented differently from Fig. 2 to better show the angle φ; the carbon atoms lie in the plane of the paper.

An effective value of $\theta=108.7°$ is unexpectedly large for an equilibrium structure which has the argon atom positioned directly above the center of mass of the propane ($\theta=90°$),

TABLE VII. Rotational constants (in MHz) of Ar propane and Ne propane calculated using the corrected propane coordinates given by Lide and using van der Waals coordinates, calculated using Kraitchman's method, and a best fit to the observed constants.

			Calculated	
		Observed[a]	Kraitchmans[b] coordinates	Best fit[c] coordinates
$Ar-C_3H_8$	*A*	7552.437	7575.28	7552.31
	B	1561.997	1556.41	1561.79
	C	1375.822	1372.27	1377.24
	rms dev		24	1
$Ar-^{13}CH_3CH_2CH_3$	*A*	7372.108	7393.51	7371.45
	B	1546.739	1540.48	1545.81
	C	1358.342	1354.32	1359.22
	rms dev		23	1
$^{20}Ne-C_3H_8$	*A*	7677.398	7677.32	
	B	2459.868	2459.65	
	C	2023.792	2023.66	
	rms dev		0.3	
$^{22}Ne-C_3H_8$	*A*	7673.46	7676.64	
	B	2322.17	2318.15	
	C	1929.39	1926.91	
	rms dev		5.7	

[a]For $Ne-C_3H_8$, the values are the average of the constants for the two internal rotor states.
[b]Calculated from coordinates obtained using Kraitchman's method. Argon coordinates: $(R_{cm},\theta,\varphi)=(3.830\text{ Å},111°,0°)$. Neon coordinates: $(R_{cm},\theta,\varphi)=(3.698\text{ Å},118.2°,2.5°)$.
[c]Coordinates adjusted to get a better fit to the rotational constants: $(R,\theta,\varphi)=(3.823\text{ Å},108.7°,0.5°)$.

but is quite reasonable for an argon equilibrium position which is equally distant from each carbon. A simple geometric calculation shows that argon will be equidistant from all three carbons when $\theta=102°$. If one acknowledges that the intermolecular interaction strength is dependent on the atomic polarizabilities, which are larger for heavier atoms, this equilibrium structure makes some sense. The difference between this and the measured value of 109° is only 7°, which is similar to the vibrationally averaged bending angle found for $Ar-CO_2$. In that complex, the equilibrium structure is T shaped and the observed angle relative to the T shape is about 9.6°.[13] Thus, the data for Ar-propane points to an equilibrium position of $\theta=102°$. Unfortunately, both the Ne-propane data and theoretical calculations disagree with this conclusion or, at least, indicate a more complicated situation.

B. Neon-propane complexes

The *A* rotational constants of $^{20}Ne-C_3H_8$ and $^{22}Ne-C_3H_8$ differ from the *C* rotational constant of propane by more than 200 MHz; this difference is only about 100 MHz in $Ar-C_3H_8$, suggesting that the neon atom is offset by a significantly greater angle from the *C* axis of the propane. Comparing the rotational constants of the ground tunneling state of $^{20}Ne-C_3H_8$ with those of C_3H_8, Kraitchman's method gives the coordinates for the neon atom in the principal axis system of the propane: $(x_\alpha, x_\beta, x_\gamma)=(0.142\ \text{Å}, 1.748\ \text{Å}, 3.256\ \text{Å})$. Thus, $(R_{cm}, \theta, \varphi)=(3.698\ \text{Å}, 118.2°, 2.5°)$. The rotational constants calculated using the neon coordinates given by Kraitchman's method are given in Table VII. In this case, the rotational constants were reproduced rather well without further adjustments, presumably because the value of x_α is not imaginary and, thus, is more reliable.

R_{cm} is 0.125 Å less for the $Ne-C_3H_8$ compared to $Ar-C_3H_8$. This is comparable to the difference of 0.129 Å found for the cyclopropane complexes.[8] The relatively large difference in θ between Ne-propane and Ar-propane (9.5°) is problematic. Using the $Rg-CO_2$ complexes again for comparison, one finds that the observed angle for $Ne-CO_2$ is only 3° larger than that for $Ar-CO_2$. The much larger difference between Ar-propane and Ne-propane suggests that, regardless of the equilibrium position, the potential energy curve along the θ coordinate is much flatter than that of the CO_2 complexes. This would produce an anomalously large bending angle for both Ar-propane and Ne-propane. Another related possibility is that these anomalous angles are related to the presence of the observable internal motion. We will investigate this further with *ab initio* calculations.

C. Tunneling motion

We found that the best fit of the Ne-propane transitions resulted when we assumed that the *c*-type transitions coincided with a change in tunneling state. This implies that the pathway between the two equivalent configurations involves an inversion of the dipole moment along the *c* axis of the complex, μ_c. Since the dipole moment of propane along its symmetry axis is predominantly responsible for the magnitude of μ_c, this can be accomplished by a rotation of the propane around its *a* axis.

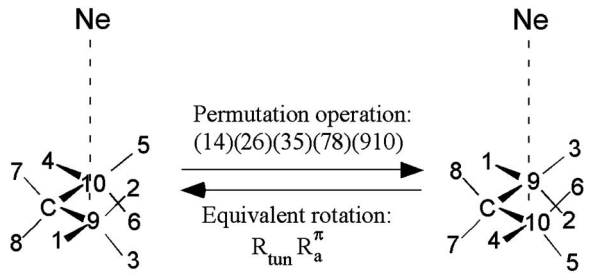

FIG. 5. Numerical labeling of the equivalent nuclei and an example of one of the permutation operations. The dotted line coincides with the *a* axis of the complex.

A group theoretical analysis shows how the presence of an internal rotation motion within the complex leads to the spectra that we observe. This analysis is similar to that done for $Ne-{}^{13}CH_2CH_2CH_2$ in which the assumed tunneling motion is a cyclopropane rotation around its symmetry axis;[8] the reader is referred to that paper and also the text by Bunker[15] for more details. Given the symmetry of the proposed structure of Ne-propane, the sets of identical nuclei are: [1,4], [2,3,5,6], [7,8], and [9,10]; the numbering of the nuclei are given in Fig. 5. There are a total of four permutation operations which result in configurations than can be obtained by overall rotation of the complex together with the specified internal rotation motion. One of the permutation operations is depicted in Fig. 5. These four operations form a group which is isomorphic with the C_{2v} molecular symmetry group, the character table for which is given in Table VIII.

The total wave function for Ne propane with an internal rotation is

$$\psi_{tot}=\psi_{elec}\psi_{vib}\psi_{rot}\psi_{nspin}\psi_{tun}. \tag{3}$$

The symmetry of this wave function must be symmetric or antisymmetric with respect to exchange of nuclei. Therefore, one finds that the reducible representation of the total wave function must be

$$\Gamma_{total}=A_1\oplus A_2. \tag{4}$$

The reducible representation of the nuclear spin states is $\Gamma_{nspin}=84A_1\oplus 52A_2\oplus 60B_1\oplus 60B_2$, and the symmetries of ψ_{elec} and ψ_{vib} are both A_1 because the complex is in the

TABLE VIII. Character table for the molecular symmetry group of Ne-propane. The complex with intermolecular tunneling has C_{2v} symmetry. The proposed tunneling path is an internal rotation of the propane within the complex. R_a^π, R_b^π, and R_c^π correspond to 180° rotations around the complex *a*, *b*, and *c* axes, respectively.

Operation				
Equivalent rotations	E R°	(14)(26)(35)(78)(910) $R_{tun}R_a^\pi$	(23)(56)(78)* $R_{tun}R_c^\pi$	(14)(25)(36)(910)* R_b^π
A_1	1	1	1	1
A_2	1	1	−1	−1
B_1	1	−1	−1	1
B_2	1	−1	1	−1

TABLE IX. Representations of the wave functions.

K_a/K_c	v	Γ_{elec}	Γ_{vib}	Γ_{rot}	Γ_{tun}	Γ_{spin}	Nuclear spin statistical weight
even/even	0	A_1	A_1	A_1	A_1	$A_1 \oplus A_2$	136
	1	A_1	A_1	A_1	B_1	$B_1 \oplus B_2$	120
even/odd	0	A_1	A_1	A_2	A_1	$A_1 \oplus A_2$	136
	1	A_1	A_1	A_2	B_1	$B_1 \oplus B_2$	120
odd/even	0	A_1	A_1	B_2	A_1	$B_1 \oplus B_2$	120
	1	A_1	A_1	B_2	B_1	$A_1 \oplus A_2$	136
odd/odd	0	A_1	A_1	B_1	A_1	$B_1 \oplus B_2$	120
	1	A_1	A_1	B_1	B_1	$A_1 \oplus A_2$	136

ground electronic and vibrational states. The reducible representation of the tunneling states is $\Gamma_{tun}=A_1 \oplus B_1$. The reducible representation of the rotational states depends on the value of the asymmetric top quantum numbers K_a and K_c. The representations for all of the wave functions are summarized in Table IX.

Since $\Gamma_{total}=\Gamma_{elec} \otimes \Gamma_{vib} \otimes \Gamma_{rot} \otimes \Gamma_{tun} \otimes \Gamma_{nspin}=A_1 \oplus A_2$, each rotational level can be associated with both tunneling states, each of which will have a different spin statistical weight. For example, for the K_aK_c=even/even levels, if $\Gamma_{tun}=A_1$, then the nuclear spin wave function can have A_1 or A_2 symmetry in order for the total wave function to have A_1 or A_2 symmetry,

$$\Gamma_{tot}=A_1 \otimes A_1 \otimes A_1 \otimes A_1 \otimes A_1=A_1,$$
$$\Gamma_{tot}=A_1 \otimes A_1 \otimes A_1 \otimes A_1 \otimes A_2=A_2. \quad (5)$$

When $\Gamma_{tun}=B_1$, then the nuclear spin wave function can have either B_1 or B_2 symmetry. The nuclear spin representations and statistical weights for the energy levels are given in Table IX.

The allowed transitions, shown in Fig. 3, are such that the nuclear spin symmetry does not change, so the allowed a-type transitions are within the tunneling states and the allowed c-type transitions change tunneling state. Thus, the splittings observed in the c-type transitions include the energy difference of the tunneling states and will be much larger than those of the a-type transitions which are governed by small differences in rotational constants. Since the splittings are unobservable for Ar-propane, ΔE must be less than or on the order of 10 kHz. This is much different from the value of ΔE=48 MHz found for ^{20}Ne-propane. This information will be valuable in our analysis of the theoretical calculations given in the next section.

V. *AB INITIO* CALCULATIONS

From the above structural analysis, we find that we cannot definitively determine the equilibrium position of the argon atom relative to the propane molecule. Yet, we do have a lot of information about the intermolecular potential. We know, for instance, that the angular orientation of the rare gas atom is unusually different in Ne-propane compared to Ar-propane. We also know that the potential is flat enough to allow internal rotation of the propane within the Ne-propane complex and that the internal rotation inverts the dipole moment of the propane. The question we pose for theoretical analysis is simple: Can a theoretical potential explain the experimental results?

Ab initio calculations were done for the Ar-propane and Ne-propane complexes to find the global and local minima and relevant barriers. One-dimensional potential curves were also mapped out in a few places. Interaction energies (E_{int}) were calculated with the supermolecular method,

$$E_{int}=\text{dimer energy-(propane energy + rare gas energy)}. \quad (6)$$

All energies were computed at the CCSD(T)/aug-cc-pVTZ level of theory (coupled-cluster with single and double excitations and noniterative triples correction/Dunning's correlation consistent-polarized valence triple zeta basis set augmented with a set of diffuse basis functions). The structure of the propane monomer was held fixed at its C_{2v} equilibrium geometry, in which the bond lengths and angles were numerically optimized in a prior calculation at the CCSD(T)/cc-pVTZ level of theory. E_{int} was corrected for basis set superposition error (BSSE) with the counterpoise method of Boys and Bernardi.[16] Computations were performed with the MOLPRO 2006.1 software package.[17]

Global and local minima in the interaction energy were found by using MOLPRO's ability to numerically minimize the BSSE-corrected interaction energies. Various initial geometries were used in the optimizations in order to locate the global and local minima. Barriers separating these minima were estimated by scanning through appropriate values of θ and ϕ while optimizing the radial coordinate R_{cm} at each θ, φ pair. Convergence of E_{int} with respect to the basis set was tested at a few geometries, including minima and barriers, by supplementing the aug-cc-pVTZ basis set with Tao's set of $3s3p2d$ bond functions halfway between the rare gas atom and the center of mass of the propane.[18] Including these functions lowered E_{int} by only 7%–8% at all test geometries, indicating that the CCSD(T)/aug-cc-pVTZ computations capture a substantial fraction of the intermolecular interaction. As examples, Table X gives optimized geometry parameters and interaction energies of the global minimum for Ar-propane and Ne-propane for the aug-cc-pVDZ and aug-

TABLE X. Equilibrium geometry and interaction energy of Rg propane as a function of basis set. The Rg is in the C_{2v} plane defined by the methylene group.

	Ar propane			Ne propane		
Basis set	R_{cm} (Å)	θ (deg)	E_{int} (cm^{-1})	R_{cm} (Å)	θ (deg)	E_{int} (cm^{-1})
aug-cc-pVDZ	3.86	91.7	−199.1	3.60	92.2	−74.2
aug-cc-pVDZ-Tao(3*s*3*p*2*d*)	3.77	91.8	−249.4	3.51	92.2	−103.1
aug-cc-pVTZ	3.74	92.3	−254.8	3.49	92.6	−105.6
aug-cc-pVTZ-Tao(3*s*3*p*2*d*)	3.72	92.0	−272.9	3.46	92.5	−114.5
aug-cc-pVQZ				3.45	92.5	−114.3

ccpVTZ basis sets and their bond function analogs. For comparison, aug-cc-pVQZ data are also included for Ne-propane; computations for Ar-propane using the aug-cc-pVQZ basis set were not carried out due to their prohibitive memory and disk requirements.

Figure 6 shows the location of the five local minima found for Ar-propane and the potential energy relative to the separate subunits. The minimized center-of-mass distances between argon and propane are also given for these minima. The global minimum has the argon atom placed above the plane of the propane carbons and shifted about 2° from the *c* axis of the propane toward the methyl groups; $(R_{cm},\theta,\varphi)=(3.740\ \text{Å},92.3°,0°)$. Ne-propane is qualitatively similar with a minimum structure of $(R_{cm},\theta,\varphi)=(3.482\ \text{Å},92.6°,0°)$. The energies of the local minima at positions (b) and (d) are similar to each other as are the energies at positions (c) and (e). This is clearly related to the number of close C–Ar interactions in a particular configuration, one in the first case and two in the second case. Thus, the position of the argon at the global minimum is due simply to the occurrence of three close C–Ar interactions at that location.

The barriers between the global minimum and local minima (b) and (d) are both high, so we can discount these as pathways for internal motion. The other two pathways, to positions (c) and (e), are more probable. The barrier to point (c) is lowest, but the reduced mass for the motion over that barrier, given by the moment of inertia around the bond axis, is more than 1.5 times higher than that for the motion over the barrier to position (e) and this results in a higher effective barrier. Thus, internal motion through position (e) is most likely, as also suggested by the experimental results.

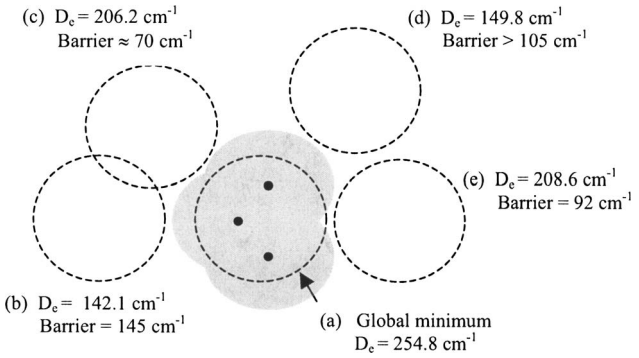

FIG. 6. This figure is drawn to show the van der Waals radii of the methyl groups, methylene group (shaded circles), and argon atoms (dotted circles). The global minimum has the argon atom above the plane of the propane carbons but slightly closer to the methyl groups than the methylene. Four additional local minima are found, all of which are in the plane of the propane carbons. The stated barriers are between the global minimum and the local minima. The coordinates for these minima are (a) $(R_{cm},\theta,\varphi)=(3.74\ \text{Å},92.3°,0°)$, (b) $(R_{cm},\theta,\varphi)=(4.468\ \text{Å},0°,0°)$, (c) $(R_{cm},\theta,\varphi)=(4.22\ \text{Å},32.5°,90°)$, (d) $(R_{cm},\theta,\varphi)=(4.91\ \text{Å},119.6°,90°)$, and (e) $(R_{cm},\theta,\varphi)=(3.967\ \text{Å},180°,0°)$.

Ignoring the propane vibrational modes, there will be three vibrational normal modes in the complex associated with the van der Waals interaction. It is likely that each mode has both angular and radial components. The fact that the equilibrium value of R_{cm} depends strongly on the angular position of the argon (see Fig. 6) is convincing theoretical evidence that the angular and radial motions are strongly coupled. We hope to do a complete vibrational analysis in the future, but to gain some insight into the dynamics of the complex now, we will consider motions in the R_{cm}, θ, and φ directions separately. In the process, we will qualitatively explain certain features of the experimental results, particularly the observed splittings in Ne-propane.

The potential energy curve for the path described by the angle θ is especially interesting because of its relationship to the proposed internal motion within the complex. *Ab initio* potential energy curves calculated for Ar-propane and Ne-propane are given in Fig. 7. φ is set at 0°, but R_{cm} is reoptimized at each value of θ in an attempt to incorporate some of the radial dependence into the potential. We see that the barriers to a motion between the two minima are 92 cm^{-1} for Ar-propane and 42 cm^{-1} for Ne-propane. A cosine series using 11 terms was fitted to the calculated points to obtain a smooth curve,

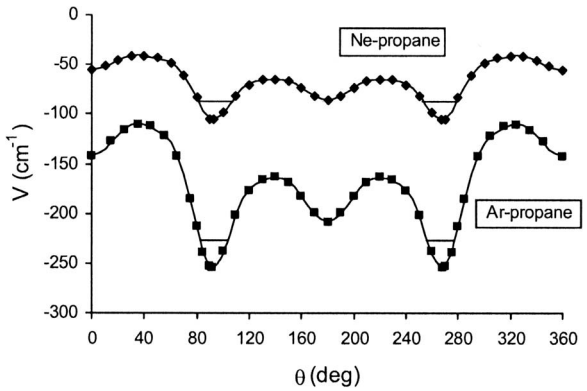

FIG. 7. The points are the results of CCSD(T)/aug-cc-pVTZ *ab initio* calculations. The curve is a cosine series function fit to the points (see text).

$$V(\theta) = \sum_{n=0}^{10} A_n \cos n\theta. \quad (7)$$

This curve was then used to calculate the vibrational energies and vibrationally averaged bending angle for the motion. If the angular motion of the argon is treated as a particle in a ring in the presence of a periodic potential $V(\theta)$, the Hamiltonian will be[10]

$$\hat{H} = -\frac{\hbar}{2I_\mu}\frac{d^2}{d\theta^2} + V(\theta), \quad \frac{1}{I_\mu} = \frac{1}{m_{\mathrm{Rg}}R_{\mathrm{cm}}^2} + \frac{1}{I_\alpha}. \quad (8)$$

The Schroedinger equation was solved using a basis set composed of the eigenfunctions for a two-dimensional rotor,

$$\psi_n(\theta) = \frac{1}{\sqrt{2\pi}} e^{\pm in\theta}.$$

Over 50 functions were needed to obtain a converged energy for the ground vibrational state of Ar-propane and over 35 were needed for Ne-propane. This large number is due to the poor choice of this basis set—the internal rotation of the propane is not well characterized as a free rotor—but it is a complete and intuitively convenient set to use. The energy of the ground vibrational state is shown as a horizontal line in Fig. 7. For Ar-propane, $D_o - D_e = 22.96\ \mathrm{cm}^{-1}$, and for Ne-propane, $D_o - D_e = 17.85\ \mathrm{cm}^{-1}$. This vibrational level is actually split into two states which are not resolvable in the figure. The energy difference between these two states is 27 kHz for Ar-propane and 39.6 MHz for Ne-propane. The splitting was also calculated for ^{22}Ne-propane and found to be 38.1 MHz. These splittings are in good qualitative agreement with our observations in which ΔE for Ar-propane is too small to be measured, $\Delta E = 48.6$ MHz for ^{20}Ne-propane, and $\Delta E = 42.1$ MHz for ^{22}Ne-propane. This is quite a sensitive test of the accuracy of the calculated potential and also suggests that the one-dimensional model of the internal motion reflects the true nature of that motion.

Rotational constants calculated from an *ab initio* equilibrium structure cannot be compared directly with experimental values because the latter result from a vibrationally averaged structure. The *ab initio* results can be corrected by calculating rotational constants for each set of R_{cm} and θ values along the potential curve given in Fig. 7, fitting a suitable function to the resulting points, and then calculating the expectation value for that function. The A rotational constant is least dependent on R_{cm}, so the expectation value for that constant, $\langle A \rangle$, will be compared to the experimental value. For Ar-propane, we find $\langle A \rangle = 7302.9$ MHz which is 250 MHz below the experimental value, and for Ne-propane, $\langle A \rangle = 7496.8$ MHz which is 180 MHz below the experimental value. Vibrationally averaged angles around the equilibrium position, derived from $\langle A \rangle$, are 6.9° for Ar-propane and 9.7° for Ne-propane. These angles are typical of van der Waals bending vibrations. For example, in the Rg–CO_2 complexes, which have T-shaped equilibrium structures, the observed bending angles are 9.60° and 7.13° away from equilibrium for Ar–CO_2 and for Ne–CO_2, respectively.[11] Unfortunately, the experimental values found for the Rg-propane complexes are much larger; using the *ab initio* equilibrium angle, the observed bending angle derived from the rotational constants is 16.4° for Ar-propane and 25.9° for Ne-propane. It is difficult to understand this discrepancy particularly when the calculated potential predicted the tunneling splitting so well.

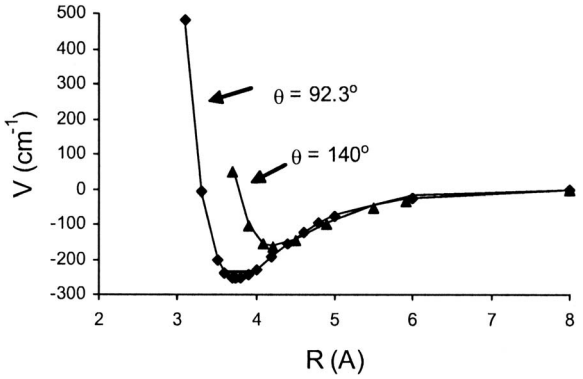

FIG. 8. Morse potential fit to the CCSD(T)/aug-cc-pVTZ *ab initio* potential. $\varphi = 0°$ and $\theta = 92.3°$ and 140°.

The radial dependence of the *ab initio* potential at a given value of θ is given in Fig. 8 for two θ values (with φ set at 0°). These curves were fit to a Morse potential function V_{Morse}, and the Schroedinger equation,

$$-\frac{\hbar^2}{2\mu}\frac{d^2\psi}{dr^2} + V_{\mathrm{Morse}}\psi = E\psi, \quad (9)$$

was solved using a shooting method[19] to find the energy of the first vibrational state and the expectation value of the argon radial position in that state. For the radial function at $\theta = 92.3°$ and $\varphi = 0°$, $\tilde{\nu} = 42\ \mathrm{cm}^{-1}$ and $\langle R^2 \rangle^{1/2} = 3.786$ Å. The value of $\tilde{\nu}$ is typical for a van der Waals stretching vibration. In fact, one obtains an experimental value of $\tilde{\nu} = 41\ \mathrm{cm}^{-1}$ calculated from the centrifugal distortion constant:[10] $\tilde{\nu} = \sqrt{4B_o^3/D_J}$. $\langle R^2 \rangle^{1/2}$ is lower than the experimental value of $R_{\mathrm{cm}} = 3.823$ Å, but, since the equilibrium value of R_{cm} gets larger as θ moves away from its equilibrium position (see Fig. 8), it is likely that an analysis that takes into account coupling of the radial and angular motions will increase R_{cm}. Values of $\tilde{\nu}$ and $\langle R^2 \rangle^{1/2}$ were also calculated for Ne-propane and were found to be 35.6 cm^{-1} and 3.592 Å, respectively. These compare to experimental values of $\tilde{\nu} = 33.4\ \mathrm{cm}^{-1}$ and $R_{\mathrm{cm}} = 3.698$ Å.

VI. RELATED WORK

In this section, we briefly compare the Rg-propane complexes with two related complexes, Rg-cyclopropane[8] and Rg-difluoromethane.[20]

A. Ar cyclopropane and Ne cyclopropane

The Rg-propane and Rg-cyclopropane systems are very similar. In both cases, the general structure has the rare gas atom positioned above the plane of the carbons. The center-of-mass van der Waals bond distances for the two systems are summarized in Table XI. R_{cm} is smaller for cyclopropane suggesting that the van der Waals bond is slightly stronger. Since Rg-cyclopropane is a symmetric top, the A rotational constant could not be determined. Therefore, the vibra-

TABLE XI. Structural parameters of Rg propane and Rg cyclopropane.

	R_{cm} (Å)	θ
$Ar-C_3H_8$	3.825	108.7°
$^{20}Ne-C_3H_8$	3.698	118.2°
$^{22}Ne-C_3H_8$	3.695	
$Ar-C_3H_6$	3.802	
$^{20}Ne-C_3H_6$	3.673	
$^{22}Ne-C_3H_6$	3.669	

tionally averaged position of the rare gas lateral to the plane of the cyclopropane carbons was not determined.

Xu and Jäger[8] observed splittings of *a*-type transitions on the order of 1 MHz in all of the Ne-cyclopropane complexes. We did not observe these transitions in Ne-propane, but they can be predicted from the measured constants and are found to be somewhat higher. For example, the splitting of the 3_{03}-2_{02} transition is predicted to be about 3.4 MHz. This suggests a lower effective barrier to the internal motion which is consistent with a lower intermolecular interaction energy in Ne-propane. Although allowed, *c*-type transitions were not observed in $Ne-{}^{13}CH_2-CH_2-CH_2$, so some details about the tunneling could not be established. The authors assumed an internal rotation around the symmetry axis of $^{13}CH_2-CH_2-CH_2$ in their discussion, but an internal rotation around an axis perpendicular to the symmetry axis, similar to what we observe in Ar-propane, would not be ruled out.

B. Ar difluoromethane

There are some interesting similarities between the $Rg-C_3H_8$ system and $Ar-CH_2F_2$.[20] In both, the argon is positioned above the plane of the heavy atoms, but away from the methylene hydrogens. In order to make a clearer comparison, we fit the observed rotational constants of $Ar-CH_2F_2$ using the same coordinate system used for $Ar-C_3H_8$. Just as in propane, the *b* axis of CH_2F_2 is the symmetry axis and the *c* axis is perpendicular to the plane of the heavy atoms. Setting $\varphi=0°$, we obtained $(R_{cm},\theta,\varphi)=(3.491\ \text{Å}, 121.92°, 0°)$ with an rms deviation of 2.8 MHz. R_{cm} is much smaller and θ is larger than that found for $Ar-C_3H_8$; both differences are presumably due to the lack of interference from methyl hydrogens in $Ar-CH_2F_2$.

The spectral features of the $Ar-CH_2F_2$ complex are very similar to those observed for $Ne-C_3H_8$ in that a set of split *c*-type transitions were measured, but the splittings are larger. In the case of $Ar-CH_2F_2$, ΔE was found to be 193 MHz. Therefore, the same type of internal motion, involving a rotation of the molecular subunit around its *a* axis, is in evidence and the barrier appears to be low, closer to that of $Ne-C_3H_8$ than $Ar-C_3H_8$. It is likely that the lower barrier in $Ar-CH_2F_2$ relative to $Ar-C_3H_8$ is also due to the lack of interference from the methyl hydrogens.

VII. CONCLUSIONS

We find that the *ab initio* calculations for Ar-propane and Ne-propane have been successful in some respects, but less so in others. The observed tunneling splittings seem to be well supported by a one-dimensional potential model. This could be fortuitous, but the idea that the internal dynamics can be viewed as a strongly hindered rotation of the propane molecule around its *a* axis seems to be accurate. We expect that extending this work to a three-dimensional analysis using the same level of *ab initio* calculations will not change this view. The calculated van der Waals bond length also seems to be reasonable. Although the vibrationally averaged values of R_{cm} were calculated to be lower than the observed values, including the angular dependence with a three-dimensional model should improve this.

The major discrepancy between theory and experiment is in the angular orientation of the argon atom relative to the propane molecule; the calculated vibrationally averaged angles are much smaller then the observed values. At this point, it is not obvious how better theoretical calculations would improve this. We have found that increasing the size of the basis set could affect the barrier height, but a lower barrier, which could increase the vibrationally averaged angle θ, would also increase the tunneling splittings. Only a dramatic change in the shape of the potential near the minimum might increase θ while keeping ΔE the same—and this would suggest a major problem with the *ab initio* results. There could be some improvement if a full three-dimensional analysis were done so that angular-radial coupling could be included in an appropriate manner. We are now in the process of doing this, because, if such an analysis does not take care of this discrepancy, we will have to look much harder at the accuracy of the calculated intermolecular potential.

ACKNOWLEDGMENTS

We would like to thank Wallace Pringle and Andrew Cooksy for extremely helpful and interesting discussions, the Petroleum Research Fund of the American Chemical Society for support, and PureBioscience (El Cajon, CA) for partial support of the computational resources.

[1] Y. Liu and W. Jäger, J. Chem. Phys. **120**, 9047 (2004).
[2] Q. Wen and W. Jäger, J. Chem. Phys. **124**, 014391 (2006).
[3] D. R. Lide, Jr., J. Chem. Phys. **33**, 1514 (1960).
[4] A. R. Hight Walker, W. Chen, S. E. Novick, B. D. Bean, and M. D. Marshall, J. Chem. Phys. **102**, 7298 (1995).
[5] F. J. Lovas and R. D. Suenram, J. Phys. Chem. Ref. Data **18**, 1310 (1989).
[6] J. K. G. Watson, *Vibrational Spectra and Structure*, edited by J. R. Durig (Elsevier, New York, 1977).
[7] H. M. Pickett, J. Mol. Spectrosc. **148**, 371 (1991); The SPCAT and SPFIT spectroscopic predicting and fitting programs are available as free downloads from http://spec.jpl.nasa.gov/
[8] Y. Xu and W. Jäger, J. Chem. Phys. **106**, 7968 (1997).
[9] J. Kraitchman, Am. J. Phys. **21**, 17 (1953).
[10] M. R. Munrow, W. C. Pringle, and S. E. Novick, J. Phys. Chem. A **103**, 2256 (1999).
[11] L. Kang, A. R. Keimowitz, M. R. Munrow, and S. E. Novick, J. Mol. Spectrosc. **213**, 122 (2002).
[12] J. Demaison and H. D. Rudolph, J. Mol. Spectrosc. **215**, 78 (2002).

[13] M. Iida, Y. Ohshima, and Y. Endo, J. Phys. Chem. **97**, 357 (1993).
[14] R. D. Suenram, G. T. Fraser, F. J. Lovas, C. W. Gillies, and J. Zozom, J. Chem. Phys. **89**, 6141 (1988).
[15] P. R. Bunker, *Molecular Symmetry and Spectroscopy* (Academic, New York, 1979).
[16] S. F. Boys and F. Bernardi, Mol. Phys. **19**, 553 (1970).
[17] H.-J. Werner, P. J. Knowles, R. Lindh *et al.*, MOLPRO, version 2006.1, a package of *ab initio* programs, see http://www.molpro.net
[18] F.-M. Tao and Y.-K. Pan, Chem. Phys. Lett. **194**, 162 (1992).
[19] W. H. Press, B. P. Flannery, S. A. Teukolsky, and W. T. Vetterling, *Numerical Recipes* (Cambridge University Press, Cambridge, England, 1989).
[20] J. Carlos López, G. Favero, A. Dell'Erba, and W. Caminati, Chem. Phys. Lett. **316**, 81 (2000).